Journal of Biomechanics 47 (2014) 323–328

Contents lists available at ScienceDirect

Journal of Biomechanics

journal homepage: www.elsevier.com/locate/jbiomech
www.JBiomech.com

Short communication

Are plasticity models required to predict relative risk of lag screw cut-out in finite element models of trochanteric fracture fixation?

Jérôme M. Goffin [a,*], Pankaj Pankaj [b], A. Hamish Simpson [a]

[a] Department of Orthopedic Surgery, The University of Edinburgh, UK
[b] School of Engineering, The University of Edinburgh, UK

ARTICLE INFO

Article history:
Accepted 8 September 2013

Keywords:
Crushable foam
Drucker–Prager
Linear elasticity
Sliding hip screw

ABSTRACT

Using a finite element model of unstable trochanteric fracture stabilized with a sliding hip screw, the benefits of two plasticity-based formulations, Drucker–Prager and crushable foam, were evaluated and compared to the commonly used linear elastic model of trabecular bone in order to predict the relative risk of lag screw cut-out for five distinct load cases. The crushable foam plasticity formulation leads to a much greater strain localization, in comparison to the other two models, with large plastic strains in a localized region. The plastic zone predicted with Drucker–Prager is relatively more diffuse. Linear elasticity associated with a minimum principal strain criterion provides the smallest volume of elements susceptible to yielding for all loading modes. The region likely to undergo plastic deformation, as predicted by the linear elastic model, is similar to that obtained from plasticity-based formulations, which indicates that this simple criterion provides an adequate estimate of the risk of cut-out.

1. Introduction

Fixation of unstable trochanteric fractures remains a challenge. One of the mechanical complications associated with such trauma surgery is migration and cut-out of the lag screw, which then requires complex salvage procedures (Weiss et al., 2012). A better understanding of the biomechanics of cut-out in trochanteric fracture fixation can minimize the risk of such complications. Finite element (FE) analysis is a powerful engineering tool which can help develop mechanics-based guidelines. FE analysis requires a constitutive model of bone. Often, researchers use linear elasticity in which the volume of elements exceeding a cut-off value (e.g. yield strain in compression) is considered to be an estimate of the region susceptible to yielding (Goffin et al., 2013a, 2013b; Schileo et al., 2008).

Beyond a critical threshold, the so-called yield stress, Hooke's law no longer holds. Use of plasticity to model the post-yield behavior of bone has attracted considerable interest (Donaldson et al., 2012a, 2012b) but has largely been overlooked in the field of orthopedic implant failure. The von Mises plasticity criterion, which does not incorporate pressure-dependent behavior of bone, has been previously used for nonlinear FE analysis (Keyak, 2001). Drucker–Prager (D–P) plasticity has been used to model bone (Bessho et al., 2007; Donaldson et al., 2008) and was calibrated using nanoindentation results on cortical bone (Mullins et al., 2009). A strain-based plasticity formulation (Pankaj and Donaldson, 2013) has also been used to predict loosening of external fixators (Donaldson et al., 2012a, 2012b). Kelly and McGarry (2012) found the pressure-dependent D–P model to be less adequate than the crushable foam plasticity formulation (CF) when trabecular bone is subjected to confined compression. The CF model was then validated as the formulation which best predicts vertebral subsidence observed experimentally in ovine lumbar vertebrae, when compared to Hill, von Mises, or D–P plasticity formulations (Kelly et al., 2013). These two plasticity models (D–P and CF) have the theoretical advantage of being pressure-dependent, and of exhibiting asymmetry in tension and compression (if crushable foam is used with volumetric hardening, i.e. CFV), which are two important features of bone. However, use of plasticity to define the constitutive law of bone significantly increases the computational effort as the problem becomes nonlinear.

Therefore, the aim of this study is to compare the relative risk of lag screw cut-out in trochanteric fracture fixation, as predicted by two relevant plasticity formulations, namely D–P and CFV, and evaluate whether the added complexity of these plasticity models is necessary for a more accurate prediction. It is hypothesized that the use of a purely linear elastic model in association with a principal strain criterion is adequate to identify whether a particular bone-implant construct is at higher risk of lag screw cut-out.

2. Materials and methods

31-A2 in the Müller AO classification labels an unstable 3-part trochanteric fracture configuration, characterized by the lack of medial support at the level of the lesser trochanter. For this purpose, a 10° wedge was removed, with an intrusion distance of 40% (Goffin et al., 2013a, 2013b), from a composite femur taken from the

* Corresponding author. Tel.: +44 131 242 6465.
E-mail address: j.goffin@ed.ac.uk (J.M. Goffin).

0021-9290/$ - see front matter
http://dx.doi.org/10.1016/j.jbiomech.2013.09.014

BEL repository (www.biomedtown.org). The fracture line was drawn at an angle of 43° with respect to the femoral shaft. A CAD model of the Omega3 Compression Hip Screw (Stryker Osteosynthesis, Schönkirchen, Germany) was inserted into the composite femur as shown in Fig. 1. A 130° 4-hole standard barrel plate was locked with Asnis III screws to the femoral shaft.

FE modeling (Abaqus/Standard 6.10-1, Simulia, Providence, Rhode Island) was used to investigate bone yielding in relation to cut-out using linear elasticity, D–P and CFV models. The femoral head was subjected to five different loading modes (Fig. 1). The stance load ('Stance') was characterized by a loading vector of magnitude 1866 N, pointing laterally in the coronal plane with an angle of 13° from the axis of the femoral shaft, and posteriorly in the saggital plane with an angle of 8° with the axis of the shaft (Eberle et al., 2009). This corresponds to the maximal loading on the hip during a walking cycle for an 80 kg person (Bergmann et al., 2001). The point of load application on the femoral head was constrained in the plane orthogonal to the loading vector while the distal femur was constrained in the three translational degrees of freedom at mid-shaft (Eberle et al., 2009).

Two fall configurations ('Fall 1' and 'Fall 2'), discussed in a previous study (Bessho et al., 2009), were also considered. 'Fall 1' features a loading vector of magnitude 3000 N parallel to the coronal plane, at an angle of 120° with respect to the femoral shaft. 'Fall 2' features torsion of the femur since the force vector of magnitude 1800 N lies at an angle of 60° with respect to the femoral shaft in the coronal plane, and points posteriorly at an angle of 45° in the transverse plane. These two cases represent extreme load variations from amongst those suggested by Bessho et al. (2009). For these two loading modes, the surface of the greater trochanter opposite the point of load application was restrained in the direction of the load (Keyak et al., 2001).

Finally, an orthotropic thermal expansion of the lag screw ('Thermal'), in the plane perpendicular to the axis of the lag screw, was employed (MacLeod et al., 2012) to model bone prestress immediately following insertion of the lag screw. Briefly, a coefficient of linear thermal expansion was set to 0.01 with a 1 °C increase in temperature corresponding to a 1% increase in screw radius. The prestressed model was then subjected to a stance load as discussed earlier ('Thermal and Stance'). Bone prestress was only modeled prior to the stance load, and not for the fall configurations, since it has been argued that time-dependent stress relaxation dissipates much of the preload (MacLeod et al., 2012) with time before a possible fall of the patient can occur.

Friction coefficients between model parts were chosen as follows: 0.46 between bone fragments (Eberle et al., 2010); 0.2 between stainless steel components (Sowmianarayanan et al., 2008); and 0.42 between bone and stainless steel (Hsu et al., 2007). The models were meshed using incompatible mode eight-node brick elements. A mesh convergence analysis was performed to ensure a sufficiently fine element discretization for strain analysis. The number of elements was varied and the displacement of the femoral head along the direction of the shaft was found to converge for an element size less than 1.5 mm (data not shown), thereby confirming the adequacy of a 1 mm hexahedral mesh.

Table 1
Material properties for different constitutive models.

Linear elastic properties for all models	
$E_{cortical}$	16 GPa
$E_{trabecular}$	155 MPa
$E_{stainless\ steel}$	195 GPa
Poisson's ratio	0.3
Linear elastic model	
Cut-off strain in compression	0.9%
Crushable foam model (CFV)	
Uniaxial to hydrostatic compression yield stress ratio	1
Hydrostatic tension to compression yield stress ratio	0.86667
Yield stress in compression	1.395 MPa
Hardening modulus	$0.05E_{trabecular}$
Drucker–Prager model (D–P)	
Friction angle	12°
Flow stress ratio	1
Dilation angle	0°
Yield stress in compression	1.395 MPa
Hardening modulus	$0.05E_{trabecular}$

The material properties used are given in Table 1. Only trabecular bone was assumed to be nonlinear for the CFV and D–P models. The cut-off strain in compression for the linear elastic model was estimated by using the yield stress in compression and Young's modulus of trabecular bone. The uniaxial to hydrostatic compression yield stress ratio of unity for CFV was based on a study by Kelly and McGarry (2012). The hydrostatic tension to compression yield stress ratio was based on uniaxial tension to compression asymmetry experimentally obtained in a previous study (Kopperdahl and Keaveny, 1998), which also results in a friction angle of 12° for D–P. These model parameters were used to conduct benchmark tests on a single cubic element model. The applied boundary conditions reproduced uniaxial (free lateral displacement, perpendicular to the direction of load application) and confined (no lateral displacement) compression tests.

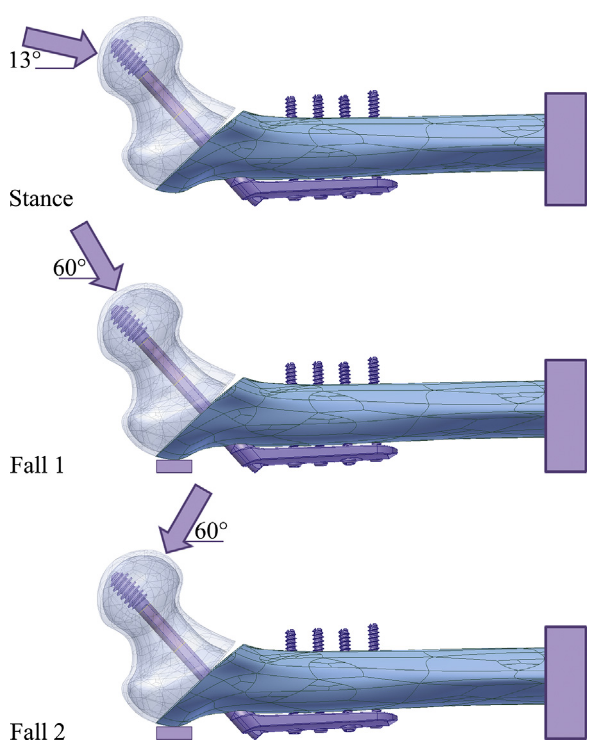

Fig. 1. Models. Sketch of the models where arrows represent the direction of the load vector in the coronal plane and rectangles depict areas where boundary conditions were applied. Three load directions were considered, i.e. a stance load and two fall configurations.

3. Results

The behavior of the cubic element modeled with in confined compression was found to closely match the results obtained with a linear elastic model (Fig. S1). This can be explained by the fact that the cone corresponding to the D–P yield surface in principal stress space becomes increasingly wider as the stress state becomes more and more compressive. For the CFV model, the post-yield behavior in confined and uniaxial compression was similar.

The extent of the plastic zone predicted by the three constitutive models is shown in Figs. 2–4 for 'Stance', 'Fall 2' and 'Thermal' load cases (for completeness, plots for 'Fall 1' and 'Thermal & Stance' are provided as Figs. S2 and S3). von Mises stress (S, Mises) and pressure (S, Pressure) are reported for all loading scenarios since the plasticity formulations considered are pressure-dependent. Minimum principal plastic strain (PE, Min. Principal) was used to delineate the plastic zone for the two plasticity models.

The volume of the predicted plastic zone (mm^3) was evaluated for the three formulations (Fig. 5) and calculated as a percentage of the volume with respect to the CFV formulation (Table 2). The evolution of the plastic zone with respect to increasing load was evaluated for 'Fall 2'; it shows that the trend depicted by Fig. 5 and Table 2 was maintained for different load magnitudes (Fig. S4). The histograms of the strain distribution in the proximal femur were derived (Fig. 6) for the two fall configurations. It shows that the strain distribution corresponding to the CFV plasticity has significantly higher plastic strain values than those for D-P or linear